Title

Ultrashort echo time magnetization transfer (UTE-MT) imaging and modeling: magic angle independent biomarkers of tissue properties

Journal

NMR in Biomedicine, 29(11)

ISSN

0952-3480

Authors

Ma, Ya-Jun
Shao, Hongda
Du, Jiang
et al.

Publication Date

2016-11-01

DOI

10.1002/nbm.3609

HHS Public Access

Author manuscript

NMR Biomed. Author manuscript; available in PMC 2017 November 01.

Published in final edited form as:

NMR Biomed. 2016 November ; 29(11): 1546–1552. doi:10.1002/nbm.3609.

Ultrashort Echo Time Magnetization Transfer (UTE-MT) Imaging and Modeling: Magic Angle Independent Biomarkers of Tissue Properties

Ya-Jun Ma[1], **Hongda Shao**[1], **Jiang Du**[1], and **Eric Y Chang**[2,1,*]

[1]Department of Radiology, University of California, San Diego, CA

[2]Radiology Service, VA San Diego Healthcare System, San Diego, CA

Abstract

Magnetic resonance (MR) imaging biomarkers such as T_2, T_2* and T_{1rho} have been widely used, but are confounded by the magic angle effect. The purpose of this study is to investigate the use of the two-dimensional ultrashort echo time magnetization transfer (UTE-MT) sequence for potential magic angle independent MR biomarkers. Magnetization transfer was investigated in cadaveric Achilles tendon samples using the UTE-MT sequence at five MT powers and five frequency offsets ranging from 2–50 kHz. The protocol was applied at 5 sample orientations ranging from 0–90° relative to the B_0 field. The results were analyzed with a two-pool quantitative MT model. Multiple TE data was also acquired and mono-exponential T_2* was calculated for each orientation. Macromolecular proton fractions and exchange rates derived from UTE-MT modeling did not appreciably change between the various orientations whereas the T_2* relaxation time demonstrated up to a 6-fold increase from 0° to 55°. The UTE-MT technique with two-pool modeling shows promise as a clinically compatible technique that is resistant to the magic angle effect. This method provides information on the macromolecular proton pool that cannot be directly obtained by other methods, including regular UTE techniques.

Graphical abstract

Graphs of T_2* values derived by fitting multiple-TE data and macromolecular proton fractions (f), T_2 value of macromolecular proton (T_{2m}) and exchange rate from macromolecular proton to water proton (RM_{0w}) derived from two-pool MT modeling with five angle orientations between fiber direction $\vec{F}$ and $\vec{B}_0$. Fitting errors of these parameters were shown by error bars.

Corresponding Author: Eric Y Chang, M.D., ericchangmd@gmail.com, VA San Diego Healthcare System, San Diego, CA 92161, Phone: 858-642-1221.

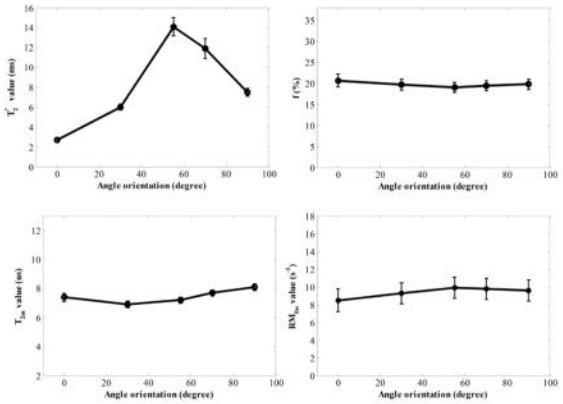

Keywords

ultrashort echo time; magnetization transfer; magic angle effect

Introduction

Over the past several decades, extensive research has been performed on the use of magnetic resonance (MR) imaging biomarkers for the evaluation of musculoskeletal tissue integrity, particularly focused on early osteoarthritis (1). T_2 and T_2* are among the most widely studied and both have been linked to alterations in the macromolecular structure of cartilage. Although nearly all commercial vendors now have standard packages that include measurements of transverse relaxation times, their routine clinical use remains limited. This is largely due to the uncertainty in the interpretation of values generated with these quantitative techniques, and a principal confounding factor is the so-called magic angle effect.

The magic angle effect is caused by changes in dipole-dipole interactions, which are minimized when tissue fiber orientation approaches 54.7° relative to the main magnetic field (2). The large orientational dependence of T_2 relaxation time in anisotropic, collagen-rich tissues has been known for more than half a century (2,3). With regards to hyaline articular cartilage, the magic angle effect is pronounced in the regions of greatest anisotropy, such as the superficial layer. For instance, studies have shown that both the T_2 and T_2* values of the superficial layer of femoral condyle cartilage obtained on clinical systems can vary by nearly 10 ms depending on the sampled location in young, asymptomatic adult volunteers (4,5). Considering that the values in these studies for the superficial layer ranged from ~45–55 ms for T_2 and ~20–50 ms for T_2*, these spatial variations account for a significant proportion of the total measurement (4,5). Furthermore, when the amount of variability in these reference values are compared with those obtained from histologically evaluated cartilage specimens, where mean differences in T_2 and T_2* of normal versus degenerated cartilage specimens also ranges from ~5–10 ms (6), it is clear that the magic angle effects rival the expected relaxation changes related to biochemical alteration and tissue compromise. In fact, previous authors have estimated that approximately 60% of the depth-wise variation of T_2 in human cartilage is accounted for by changes in collagen anisotropy (7). Studies that have

investigated T_{1rho} using traditional, continuous wave spin-lock pulses in cartilage have found similar results, whereby dipolar interaction is the dominant relaxation mechanism and therefore measurements are exquisitely sensitive to the magic angle effect (8).

Magnetization transfer (MT) imaging is an indirect technique that has been used to provide information on proton pools with extremely fast transverse relaxation (9). In a two-pool MT model, contrast is based on interactions between macromolecular and water protons. Specifically, saturation pulses transmitted at a radiofrequency off the main water proton frequency will preferentially affect the macromolecular proton pool. The saturated macromolecular protons will subsequently transfer magnetization to the water proton pool and imaging of the decreased water proton signal will provide information on these interactions when compared with an unsaturated image. MT measures have shown promise as MR biomarkers in longer T2 structures such as cartilage, including sensitivity to changes in macromolecules (10). MT has also been shown to have much less orientational dependence compared with T_2 relaxation measurements (11). While MT can be used to indirectly study macromolecular proton pools, conventional acquisition methods are limited with regards to acquiring adequate signal from tissues with short mean transverse relaxation times.

In recent years, ultrashort echo time (UTE) sequences have been used to study tissues or tissue components with short transverse relaxation times, which result in little or no signal when imaged using conventional MR sequences. Tendon is one such tissue, where the highly anisotropic structure of collagen and relatively low hydration results in short mean transverse relaxation times. The magic angle effect has a proportionally larger impact on these highly anisotropic tissues and authors have shown a 37-fold increase in T_2, 10-fold increase in UTE-T_2*, and 7-fold increase in UTE-T_{1rho} with tendon specimen orientation from 0° to 55° relative to the main magnetic field (12–15). Use of the UTE sequence shows promise in that it allows for signal detection and quantification of otherwise “invisible” tendon when imaged using clinical MR sequences (16). However, the need for the development and validation of less magic angle dependent MR biomarkers for short T_2 tissues is clear. The purpose of our study is to investigate the use of the two-dimensional UTE magnetization transfer (UTE-MT) sequence with two-pool modeling for the potential magic angle independent assessment of tissue properties.

Materials and methods

Sample Preparation and Imaging Parameters

Human Achilles tendon samples dissected from four fresh cadaveric ankle specimens were harvested for this study. Data were acquired with a 2D UTE-MT sequence on a clinical 3T Signa TwinSpeed scanner (GE Healthcare Technologies, Milwaukee, WI) with a maximum gradient strength of 40 mT/m and a maximum slew rate of 150 mT/m/ms. A home-built birdcage coil (~2 cm in diameter) was used for signal excitation and reception. The UTE-MT sequence employed a short non-selective hard pulse (duration = 16μs) excitation followed by 2D radial ramp sampling with a minimal nominal TE of 8μs. The MT preparation is consisted of a Fermi shaped radiofrequency (RF) pulse (duration = 8 ms, bandwidth is 160Hz) followed by a gradient crusher. The area ratio of the MT pulse to a

rectangular pulse with the same duration and peak amplitude is 0.59. The UTE-MT imaging protocol included: TR = 50 ms, TE = 8 μs, Flip angle = 5°, FOV = 5 × 5 cm^2, matrix = 256 × 256; one MT pulse per TR, five MT powers (300°, 600°, 900°, 1200° and 1500°) and five MT frequency offsets (2, 5, 10, 20 and 50 kHz), with a total of 25 different MT datasets and the total scan time was 17.5min. The peak B_1 value of MT pulse in 1500° is 20.7uT. The same protocol was applied to each tendon sample five times, with the sample oriented 0°, 30°, 55°, 70° and 90° relative to the B_0 field. Multiple TE data was also acquired with these five angle orientations for mono-exponential fitting to determine T_2* value of the water component. The protocol for multiple-TE data acquisition was identical with the UTE-MT protocol except that a non-MT pulse was used and TEs were 0.008, 2, 4, 8, 12, 16, 20 ms with a total scan time of 4.9min.

Pre-measurement of T_1 values is necessary for MT modeling. A multiple-TR UTE protocol was employed for T_1 measurement, whose sequence parameters were the same with the MT modeling protocol except that a no MT pulse was used, image flip angle = 25°, and TRs were 25, 50, 100, 200, 400, 600 ms. The total scan time for T_1 measurement was 9.2min. Previous work has shown that T_1 is resistant to the magic angle effect (11), and therefore the multiple-TR sequence was only performed with angle orientation = 55° for each sample. Thus, total scan time for MT modeling including the T_1 measurement and MT sequences are 26.7min.

Image and Data Analysis

Two-pool UTE-MT modeling was performed on the datasets as previously described by Ramani et al (17). Ramani et al introduced a simple method by treating the MT pulse as a rectangular continuous wave (CW) signal with the same mean saturating power as the experimentally used shaped pulse in each repetition time, the so-called continuous wave power equivalent (CWPE) approximation. W_{CWPE} is the angular frequency of precession induced by the off-resonance MT pulse and is a measure of the amplitude of the B_1 field, as represented by:

$$w_{\mathrm{CWPE}}=\frac{\theta_{\mathrm{sat}}\pi}{p_1 180^\circ}\sqrt{\frac{p_2}{\tau_{sat}TR}}, \quad [1]$$

where θ_{sat} is the flip-angle of MT pulse. p_1 is the ratio of the area of the MT pulse to a rectangular pulse with the same duration and peak amplitude and p_2 is the ratio of the square of the MT pulse area to the square of the area of the same rectangular pulse. $\tau_{sat;}$ is the duration of the MT pulse, and TR is the time interval between adjacent two MT pulses. The acquired data with a variety of saturation powers and off-resonance frequencies Δf were fitted by the Ramani model where the signal intensity S is given by:

$$S=gM_{0w}\frac{R_{1m}\left[\frac{RM_{0w}f}{R_{1w}(1-f)}\right]+R_{RFm}+R_{1m}+RM_{0w}}{\left[\frac{RM_{0w}f}{R_{1w}(1-f)}\right](R_{1m}+R_{RFm})+\left(1+\left[\frac{w_{\mathrm{CWPE}}}{2\pi\Delta f}\right]^2\left[\frac{1}{R_{1w}T_{2w}}+\right]\right)(R_{RFm}+R_{1m}+RM_{0w})} \quad [2]$$

where g is a amplitude scaling factor of the acquired data including the item of exp(−TE/T_2*). f is the macromolecular proton fraction, i.e. $f=\frac{M_{0m}}{M_{0m}+M_{0w}}$. M_{0m} and M_{0w} are the fully relaxed magnetization of macromolecular pool and water pool respectively. R_{1m} and R_{1w} are the longitudinal rate constants, respectively. R is the first-order magnetization exchange rate constant between the two pools. R_{RFm} is the loss rate of longitudinal magnetization of macromolecular pool due to the RF saturation of the MT pulse. It is related to the absorption lineshape G(2πΔf) of the spins in the macromolecular pool and is given by:

$$R_{RFm}=\pi w_{\mathrm{CWPE}}^2\mathrm{G}(2\pi\Delta\mathrm{f}). \quad [3]$$

Since the protons in the macromolecular pool do not experience the motional narrowing that the protons in the free pool experience, they cannot be characterized by the Lorentzian lineshape function that results from the Bloch formalism. Super-Lorentzian lineshapes have been reported to be good representations for the macromolecular pool in Achilles tendon (18). The super-Lorentzian expression is as follows:

$$G(2\pi\Delta\mathrm{f})=\int_0^{\pi/2}d\theta\sin\theta\sqrt{\frac{2}{3}}\frac{T_{2m}}{|3\cos^2\theta-1|}\exp\left(-2\left[\frac{2\pi\Delta fT_{2m}}{|3\cos^2\theta-1|}\right]^2\right), \quad [4]$$

where θ is the angle orientation between the axis of molecular orientation and the B_0.

Then, if the apparent longitudinal relaxation rate $R_{1\mathrm{obs}}$ (= $1/T_1$), which can be measured by a conventional T_1 measurement sequence such as multiple-TR UTE protocol mentioned above, is known, $R_{1\mathrm{w}}$is determined by (17,18):

$$R_{1\mathrm{w}}=\frac{R_{1\mathrm{obs}}}{1+\frac{\frac{RM_{0w}f}{R_{1w}(1-f)}(R_{1m}-R_{1\mathrm{obs}})}{(R_{1m}-R_{1\mathrm{obs}})+RM_{0w}}}. \quad [5]$$

Since the quantitative MT experiments are largely insensitive to R_{1m} (i.e. the relaxation rate of the macromolecular pool), R_{1m} has been fixed arbitrarily to be $1\mathrm{s}^{-1}$(17–19). Above all, acquired MT data can be fitted to Eq. [2] with the information of Eq. [1] and Eq. [3] to Eq. [6]. Thus, the parameters including f, RM_{0w} and T_{2m} can be determined by this fitting

procedure. RM_{0w} is the proton exchange rate from macromolecular to water. The residual of fitting was represented by $\text{Residual}=\sqrt{\frac{\sum_i (S_{i,fit}-S_i)^2}{\sum_i S_i^2}}$, where, S_i, $S_{i,fit}$ (i=1,…,N, N is the total number of data points in one MT datasets) are the experimental and fitted data points.

The analysis algorithm was written in Matlab (The MathWorks Inc., Natick, MA, USA) and was executed offline on the DICOM images obtained by the protocols described above. A Levenberg-Marquardt algorithm was employed for the nonlinear least-squares fitting in both MT modeling and multiple-TE mono-exponential fitting. The program allowed placement of region of interests (ROIs) on the first UTE image of the series, which were then copied onto each of the subsequent images. The mean intensity within each of the ROIs was used for both two-pool modeling and multiple-TE mono-exponential fitting.

Results

Figure 1 shows UTE-MT images of a cadaveric human Achilles tendon sample acquired at five angular orientations (i.e. 0°, 30°, 55°, 70°, 90°) between fiber direction and the B_0 field. Using the UTE sequence, high signal intensity is obtained from the Achilles tendon all images at all angular orientations, facilitating MT modeling as conventional clinical sequences show near zero signal, thereby limiting MT modeling. The image intensity increased with higher off-resonance frequencies due to reduced saturation of macromolecular spins. Signal intensity varied depending on orientation and the greatest signal was observed for the Achilles tendon when the fibers were oriented near the magic angle of 55°. T_2* also was significantly increased near the magic angle due to the minimization of dipole-dipole interaction.

Figure 2 shows the results of both UTE-MT modeling and multiple-TE T_2* fitting. The measured T_1 value of this sample was 698ms. The two-pool UTE-MT modeling provides excellent fitting (all Residuals were less than 2.1%) of signal changes over five MT power (i.e. 300°, 600°, 900°, 1200° and 1500°) and five off-resonance frequencies (i.e. 2, 5, 10, 20, 50 KHz). Furthermore, the UTE-MT modeling performed well for all five angular orientations (i.e. 0°, 30°, 55°, 70° and 90°), thereby allowing direct comparison of values at each orientation. Excellent T_2* fitting was also achieved for all five angular orientations, allowing quantitative comparison of the angular dependence of UTE-MT modeling and T_2* relaxation time.

Figure 3 shows the relationship of UTE-MT modeling parameters and T_2* relaxation time with respect to angular orientation in a representative cadaveric human Achilles tendon sample. As can be seen, T_{2w}* shows a strong magic angle behavior, with ~6 times increase from 2.5 ms when the sample was oriented parallel to the B_0 field, to 14.8 ms when the sample was oriented 55° relative to the B_0 field. Meanwhile, the UTE-MT modeling parameters, including macromolecular proton fractions (f), T_2 value of macromolecular proton (T_{2m}) and exchange rate from macromolecular proton to water proton (RM_{0w}) derived from MT modeling, all show minimal angular dependence with less than 10%

variation. These results suggest that the f, T_{2m} and RM_{0w} can be used as magic angle insensitive biomarkers of the Achilles tendon.

Table 1 shows the mean and coefficient of variation (CV) values of f, T_{2m}, RM_{0w} and T_2* across five angle orientations between fiber direction $\vec{F}$ and $\vec{B}_0$ of four cadaveric human Achilles tendon samples. CV is a statistical measure defined as the dispersion of data points in a data series around the mean. It is calculated as follows: (standard deviation) / (mean value). The small CV values of f, T_{2m} and RM_{0w} in all the four samples show magic angle independent results from MT modeling. In contrast, the relatively large CV values of T_2* show its magic angle sensitivity.

Discussion

In this study, we have shown that UTE-MT modeling can be performed on data acquired on a clinical 3T scanner and provides parameters that are resistant to the magic angle effect, such as macromolecular proton fractions and exchange rates between water and macromolecular protons. This contrasts with the exquisitely magic-angle sensitive mono-exponential UTE-T_2* relaxation times, which demonstrated up to a 6-fold increase from 0° to 55° in our tendon specimens, a finding similar to previously published results (13,14).

Henkelman et al were among the first to show that MT demonstrated no orientation dependence (11). Their experiments were performed on a variety of tissues, including tendon and cartilage, and the classic two-pool MT model introduced by the same group was used for fitting (11,19). However, their sequence and model utilized a long continuous MT RF pulse to drive the two-pool system to the steady state and was employed on an NMR spectrometer. This method may not be possible with clinical MR imaging hardware systems due to very large specific absorption rates (SAR). To accomplish MT imaging on a conventional clinical scanner, Ramani et al employed a continuous wave power equivalent method for pulsed wave saturation and were able to fit a number of parameters such as the T_2 values of both water (T_{2w}) and macromolecular protons (T_{2m}), macromolecular proton fractions (f), proton exchange rates from macromolecular to water (RM_{0w}) pools (17). Using the UTE-MT technique and Ramani model on a clinical 1.5T system, Hodgson et al found a bound proton fraction of 21.0 ± 1.2% versus 16.4% in the Achilles tendons of eight volunteers and a psoriatic arthritis patient, respectively ($p < 0.05$) (18). The bound proton fractions in our specimens (19–21%) are comparable to those reported in healthy volunteers (18) and is in keeping with the high collagen content of the Achilles tendon, which has been reported at 22% of the total tendon wet weight (20).

In recent years, a number of potential clinically compatible, magic angle resistant MR biomarkers have been proposed. This includes T_{1rho} using an adiabatic spin-lock RF pulse (21,22), UTE-T_2* bi-component fractions (23,24), and diffusion weighted imaging (25). Our results confirm that UTE-MT also yields magic-angle independent measurements. Compared with the other techniques, a unique advantage of the UTE-MT sequence is that information on the macromolecular protons can be obtained. This proton pool typically demonstrates extremely rapid T_2 relaxation and cannot be directly obtained by other clinically compatible methods, including UTE or zero echo time (ZTE) techniques. The

combination of UTE-MT modeling measurements with UTE-T_2* bi-component fractions would be of interest to provide information on all proton pools, including macromolecular protons, bound water, and free water. This along with correlation with physical and biomechanical measurements will be investigated in future work.

In this study, we used a home-built birdcage coil (~2 cm in diameter) for signal transmission and receiving, which has excellent transmission efficiency. The SAR values were very low, but cannot be compared with the in vivo condition. In particular, SAR values can be quite different with different body parts and transmission coils despite similar protocols. For example, to image a human leg in vivo, the SAR value of the UTE-MT protocol with a MT power of 1400° and TR = 100 ms is close to the SAR limitation.

Our study has a number of limitations. First, we had a small sample size without histologic correlation. In severely degenerated tendons, collagen fibers are disrupted, collagen content decreases, and water increases. In this setting, the degree of magic angle effect on T_2 times may decrease slightly, but would still be expected to be present. Second, the imaging parameters used in this study are prohibitively long for clinical translation (i.e. 26.7min for one slice). We have tried MT modeling with as few as ten datasets and the results were comparable to those obtained using all 25 datasets. Alternatively, an optimal data acquisition scheme using the theory of Cramer-Rao lower bounds (CRLB) to select MT powers and frequency offsets for MT modeling can be employed to reduce scan time (26). Furthermore, the scan time of the T_1 measurement sequence can also be decreased by reducing the number of TR or TR values. Overall, there is ample opportunity to reduce scan time for clinical use, although the limits of reducing datasets remain to be fully studied. In particular, with reduced datasets, the fitting can be more sensitive to noise or image artifacts caused by off-resonance or motion. Third, although the image flip angle used in this study was very small (i.e. 5°), a bias was still introduced into the Ramani MT model due to T_1 weighting and on-resonance saturation. In addition, the relatively small saturation pulse duty cycle of the UTE-MT protocol may lead to substantial underestimation of the exchange rate between macromolecular and water pools, creating inaccuracy in the measurement of T_{2w}. Alternative models that consider the excitation pulse and repetition time are less sensitive to T_1 weighting (27).

In conclusion, UTE-MT modeling provides information on tissue properties, such as the macromolecular proton fraction and exchange rates between water and macromolecular protons, and is much less sensitive to the magic angle effect compared with mono-exponential T_2* values of the water protons. UTE-MT modeling can be applied to both short and long T_2 tissues such as the Achilles tendon, ligaments, menisci, bone, calcified cartilage and superficial layers of cartilage, and may be potentially be useful for disease identification, monitoring disease progression, and assessing response to therapy.

Acknowledgments

The authors acknowledge grant support from NIH (1R01 AR062581 and 1R01 AR068987) and the VA Clinical Science R&D Service (5IK2CX000749 and 1I01CX001388).

Abbreviations used

MR	magnetic resonance
UTE	Ultrashort echo time
RF	radiofrequency
UTE-MT	UTE magnetization transfer
CW	continuous wave
CWPE	continuous wave power equivalent
ROIs	region of interests
CV	coefficient of variation
SAR	specific absorption rates
ZTE	zero echo time
CRLB	Cramer-Rao lower bounds

References

1. Binks DA, Hodgson RJ, Ries ME, Foster RJ, Smye SW, McGonagle D, Radjenovic A. Quantitative parametric MRI of articular cartilage: a review of progress and open challenges. Br J Radiol. 2013; 86(1023):20120163. [PubMed: 23407427]
2. Xia Y. Magic-angle effect in magnetic resonance imaging of articular cartilage - A review. Invest Radiol. 2000; 35(10):602–621. [PubMed: 11041155]
3. Berendsen HJC. Nuclear Magnetic Resonance Study of Collagen Hydration. J Chem Phys. 1962; 36(12):3297–&.
4. Hannila I, Raina SS, Tervonen O, Ojala R, Nieminen MT. Topographical variation of T2 relaxation time in the young adult knee cartilage at 1. 5 T. Osteoarthr Cartilage. 2009; 17(12):1570–1575.
5. Bittersohl B, Hosalkar HS, Sondern M, Miese FR, Antoch G, Krauspe R, Zilkens C. Spectrum of T2*values in knee joint cartilage at 3 T: a cross-sectional analysis in asymptomatic young adult volunteers. Skeletal Radiol. 2014; 43(4):443–452. [PubMed: 24425347]
6. Kim T, Min BH, Yoon SH, Kim H, Park S, Lee HY, Kwack KS. An in vitro comparative study of T2 and T2* mappings of human articular cartilage at 3-Tesla MRI using histology as the standard of reference. Skeletal Radiol. 2014; 43(7):947–954. [PubMed: 24715200]
7. Nissi MJ, Rieppo J, Toyras J, Laasanen MS, Kiviranta I, Jurvelin JS, Nieminen MT. T(2) relaxation time mapping reveals age- and species-related diversity of collagen network architecture in articular cartilage. Osteoarthritis Cartilage. 2006; 14(12):1265–1271. [PubMed: 16843689]
8. Mlynarik V, Szomolanyi P, Toffanin R, Vittur F, Trattnig S. Transverse relaxation mechanisms in articular cartilage. J Magn Reson. 2004; 169(2):300–307. [PubMed: 15261626]
9. Henkelman RM, Stanisz GJ, Graham SJ. Magnetization transfer in MRI: a review. NMR Biomed. 2001; 14(2):57–64. [PubMed: 11320533]
10. Gray ML, Burstein D, Lesperance LM, Gehrke L. Magnetization transfer in cartilage and its constituent macromolecules. Magn Reson Med. 1995; 34(3):319–325. [PubMed: 7500869]
11. Henkelman RM, Stanisz GJ, Kim JK, Bronskill MJ. Anisotropy of NMR properties of tissues. Magn Reson Med. 1994; 32(5):592–601. [PubMed: 7808260]
12. Fullerton GD, Cameron IL, Ord VA. Orientation of Tendons in the Magnetic-Field and Its Effect on T2 Relaxation-Times. Radiology. 1985; 155(2):433–435. [PubMed: 3983395]

13. Du J, Chiang AJT, Chung CB, Statum S, Znamirowski R, Takahashi A, Bydder GM. Orientational analysis of the Achilles tendon and enthesis using an ultrashort echo time spectroscopic imaging sequence. Magnetic Resonance Imaging. 2010; 28(2):178–184. [PubMed: 19695811]
14. Du J, Statum S, Znamirowski R, Bydder GM, Chung CB. Ultrashort TE T1rho magic angle imaging. Magn Reson Med. 2013; 69(3):682–687. [PubMed: 22539354]
15. Krasnosselskaia LV, Fullerton GD, Dodd SJ, Cameron IL. Water in tendon: Orientational analysis of the free induction decay. Magnet Reson Med. 2005; 54(2):280–288.
16. Chang EY, Du J, Bae WC, Chung CB. Qualitative and Quantitative Ultrashort Echo Time Imaging of Musculoskeletal Tissues. Semin Musculoskelet Radiol. 2015; 19(4):375–386. [PubMed: 26583365]
17. Ramani A, Dalton C, Miller DH, Tofts PS, Barker GJ. Precise estimate of fundamental in-vivo MT parameters in human brain in clinically feasible times. Magn Reson Imaging. 2002; 20(10):721–731. [PubMed: 12591568]
18. Hodgson RJ, Evans R, Wright P, Grainger AJ, O'Connor PJ, Helliwell P, McGonagle D, Emery P, Robson MD. Quantitative magnetization transfer ultrashort echo time imaging of the Achilles tendon. Magn Reson Med. 2011; 65(5):1372–1376. [PubMed: 21500263]
19. Henkelman RM, Huang X, Xiang QS, Stanisz GJ, Swanson SD, Bronskill MJ. Quantitative interpretation of magnetization transfer. Magn Reson Med. 1993; 29(6):759–766. [PubMed: 8350718]
20. de Mos M, van El B, DeGroot J, Jahr H, van Schie HT, van Arkel ER, Tol H, Heijboer R, van Osch GJ, Verhaar JA. Achilles tendinosis: changes in biochemical composition and collagen turnover rate. Am J Sports Med. 2007; 35(9):1549–1556. [PubMed: 17478653]
21. Rautiainen J, Nissi MJ, Liimatainen T, Herzog W, Korhonen RK, Nieminen MT. Adiabatic rotating frame relaxation of MRI reveals early cartilage degeneration in a rabbit model of anterior cruciate ligament transection. Osteoarthritis Cartilage. 2014; 22(10):1444–1452. [PubMed: 25278055]
22. Zhang J, Nissi MJ, Idiyatullin D, Michaeli S, Garwood M, Ellermann J. Capturing fast relaxing spins with SWIFT adiabatic rotating frame spin-lattice relaxation (T) mapping. NMR Biomed. 2016
23. Shao H, Chang EY, Pauli C, Zanganeh S, Bae W, Chung CB, Tang G, Du J. UTE bi-component analysis of T2* relaxation in articular cartilage. Osteoarthritis Cartilage. 2016; 24(2):364–373. [PubMed: 26382110]
24. Pauli C, Bae WC, Lee M, Lotz M, Bydder GM, D'Lima DL, Chung CB, Du J. Ultrashort-echo time MR imaging of the patella with bicomponent analysis: correlation with histopathologic and polarized light microscopic findings. Radiology. 2012; 264(2):484–493. [PubMed: 22653187]
25. Szczepankiewicz F, Lasic S, van Westen D, Sundgren PC, Englund E, Westin CF, Stahlberg F, Latt J, Topgaard D, Nilsson M. Quantification of microscopic diffusion anisotropy disentangles effects of orientation dispersion from microstructure: applications in healthy volunteers and in brain tumors. Neuroimage. 2015; 104:241–252. [PubMed: 25284306]
26. Cercignani M, Alexander DC. Optimal acquisition schemes for in vivo quantitative magnetization transfer MRI. Magn Reson Med. 2006; 56(4):803–810. [PubMed: 16902982]
27. Cercignani M, Barker GJ. A comparison between equations describing in vivo MT: The effects of noise and sequence parameters. J Magn Reson. 2008; 191(2):171–183. [PubMed: 18191599]

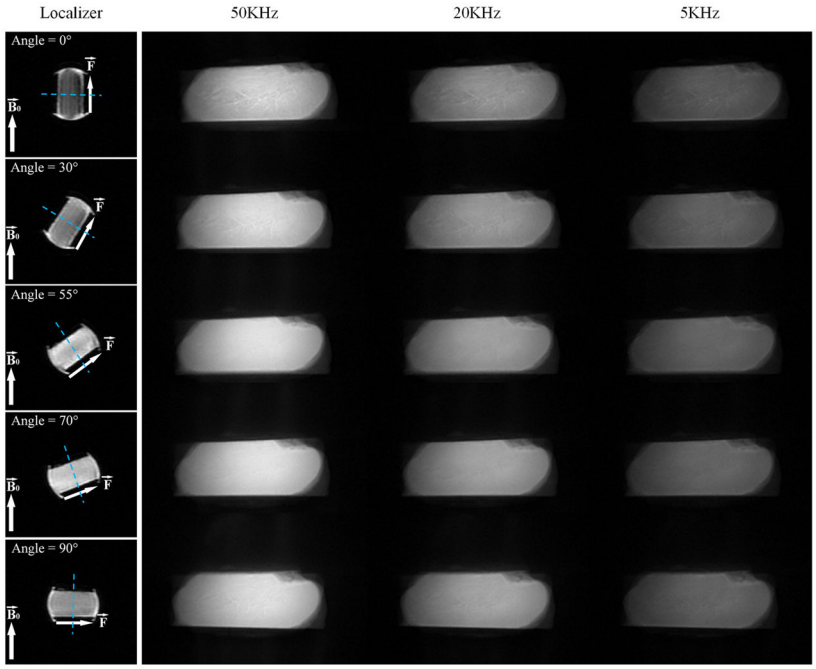

Figure 1.

Localizers and MT images of five angle orientations (i.e. 0°, 30°, 55°, 70°, 90°) between fiber direction $\vec{F}$ and main field $\vec{B}_0$. The localizer sequence was the conventional GRE sequence with TE/TR=3.2/8.6ms. The first columns are the images of localizers and the direction of both $\vec{F}$ and $\vec{B}_0$ are represented by white arrows. The blue dashed lines are the imaging planes. The second to fourth columns are the corresponding MT images with off-resonance frenquencies of 50, 20 and 5KHz and a flip angle of 1200°. Each row of MT images with the same angle orientation are normlized by themselves.

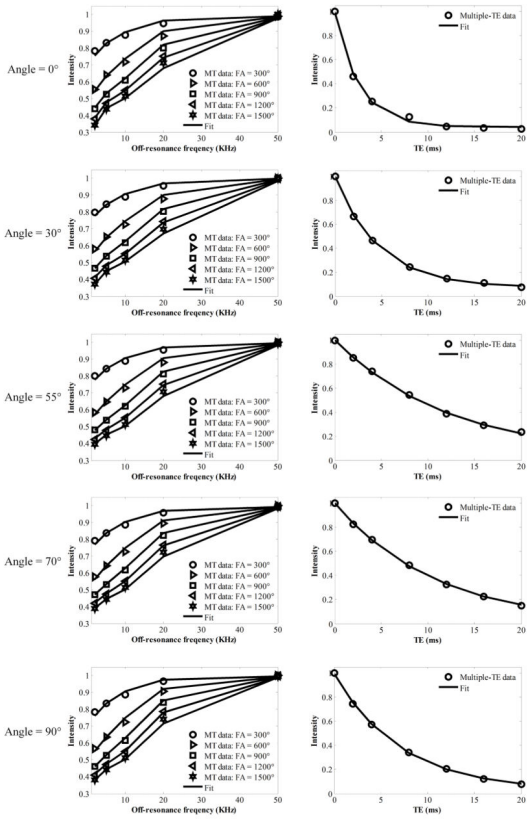

Figure 2.

Graphs of fitting results of both MT modeling (first column) and multiple-TE data (second column). The results of five angle orientations between fiber direction $\vec{F}$ and $\vec{B_0}$ are shown in the first to fifth rows, respectively.

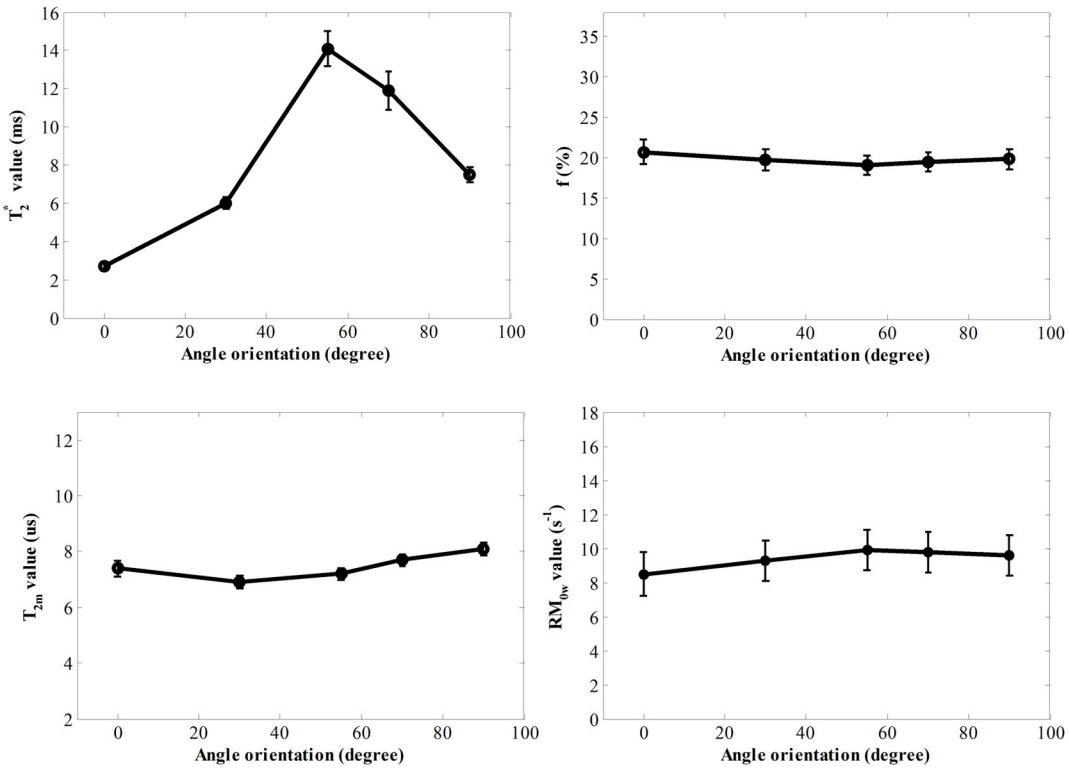

Figure 3.

Graphes of T_2* values derived by fitting multiple-TE data and macromolecular proton fractions (f), T_2 value of macromolecular proton (T_{2m}) and exchange rate from macromolecular proton to water proton (RM_{0w}) derived from two-pool MT modeling with five angle orientations between fiber direction $\vec{F}$ and $\vec{B}_0$. Fitting errors of these parameters were shown by error bars.

Table 1

Mean and coefficient of variation (CV) values of f, T_{2m}, and RM_{0w} derived by two-pool MT modeling and T_2* derived by multiple-TE data fitting across five angle orientations (i.e. 0°, 30°, 55°, 70°, 90°) between fiber direction $\vec{F}$ and $\vec{B}_0$ of four Achilles tendons.

Sample	f (%)	T_{2m} (us)	RM_{0w} (s^{-1})	T2*(ms)
1	19.8±3.0%	7.5±6.7%	9.4±6.4%	8.4±54.8%
2	19.9±3.0%	7.6±7.9%	16.7±6.6%	5.9±69.5%
3	19.6±3.1%	7.2±6.9%	10.6±7.5%	5.6±66.1%
4	20.0±1.5%	7.6±9.2%	9.2±2.2%	6.1±75.4%